

# 1 **Wetland loss in the Ñeembucú Wetlands Complex, Paraguay, using remote sensing**

2 Frances O’Leary<sup>1</sup>

3 <sup>1</sup> Para La Tierra, Centro IDEAL, Mariscal Estigarribia 321 c/ Tte. Capurro, Pilar, Dpto.  
4 Ñeembucú, Paraguay.

5

## 6 **Abstract**

7 South American wetlands are of global importance, yet limited delineation and  
8 monitoring restricts informed decision-making around the drivers of wetland loss. A  
9 growing human population and increasing demand for agricultural products has driven  
10 wetland loss and degradation in the Neotropics. Understanding of wetland dynamics  
11 and land use change can be gained through wetland monitoring. The Ñeembucú  
12 Wetlands Complex is the largest wetland in Paraguay, lying within the Paraguay-  
13 Paraná-La Plata River system. This study aims to use remotely sensed data to map land  
14 cover between 2006 and 2021, quantify wetland change over the 15-year study period  
15 and thus identify land cover types vulnerable to change in the Ñeembucú Wetlands  
16 Complex. Forest, dryland vegetation, vegetated wetland and open water were identified  
17 using Random Forest supervised classifications trained on visual inspection data and  
18 field data. Annual change of -0.34, 4.95, -1.65, 0.40 was observed for forest, dryland,  
19 vegetated wetland and open water, respectively. Wetland and forest conversion is  
20 attributed to agricultural and urban expansion. With ongoing pressures on wetlands,  
21 monitoring will be a key tool for addressing change and advising decision-making  
22 around development and conservation of valuable ecosystem goods and services in the  
23 Ñeembucú Wetlands Complex.

24

## 25 **Additional Keywords**

26 Remote sensing, Paraguay, Paraná, La Plata, land use change, wetland conversion,  
27 neotropics

28

## 29 **1. Introduction**

30 South American wetlands are of global importance, yet limited delineation and  
31 monitoring restricts informed decision-making around the drivers of wetland loss in the

32 neotropics. Wetlands are some of the most valuable ecosystems on Earth, providing  
33 goods and services including water storage and purification, carbon fixation,  
34 agricultural production and provision of biodiverse habitat (Kashaigili et al., 2006;  
35 Ramsar Convention, 2016; Guo et al., 2017). Wetlands are estimated to cover around 3-  
36 6% of the Earth's surface and South America holds a large proportion of these, with  
37 wetland area covering 20% of the continent's surface and holding 42% of the Earth's  
38 peat volume (Junk, 2013; Gumbrecht et al., 2017; Kandus et al., 2018).

39 Despite their value, wetlands are one of the Earth's most vulnerable ecosystems  
40 (Millennium Ecosystem Assessment, 2005). Wetlands are being lost at a faster rate than  
41 any other ecosystem, with over half of Earth's wetlands becoming degraded or lost in  
42 the last 150 years (Sica et al., 2016; Slagter et al., 2020). Wetland degradation,  
43 destruction and modification has been driven by anthropogenic and natural pressures  
44 (Baker et al., 2007; Gardner et al., 2015; Reis et al., 2017). In South America, a growing  
45 human population and increasing demand for agricultural products has driven  
46 infrastructure development, agricultural expansion and exploitation of natural resources,  
47 exerting pressure on wetlands. Extreme weather events such as drought and storms can  
48 also drive wetland change. Wetland destruction and degradation reduces the capacity of  
49 wetlands to provide valuable ecosystem services, including reduced flood and drought  
50 mitigation, wetland biodiversity loss, and reduced provisioning of natural resources.

51 Despite global concern for wetland habitats and the ecosystem goods and services they  
52 provide, little is known about the extent of wetland conversion in South America (Junk,  
53 2013). Paraguay is one of South America's least studied countries, and even less is  
54 known about the largest wetland within Paraguay's administrative boundaries, the  
55 Ñeembucú Wetlands Complex (Kandus et al., 2018; Pett and Wyer, 2020; Rosset et al.,  
56 2020). The Ñeembucú Wetlands Complex lies within the Paraguay-Paraná-La Plata  
57 River system, which has the 9<sup>th</sup> highest water discharge into oceans and 5<sup>th</sup> highest  
58 drainage area of rivers worldwide (Milliman and Meade, 1983; Junk, 2013). The  
59 Paraguay-Paraná-La Plata River system flows from tropical to temperate regions,  
60 resulting in high environmental heterogeneity and biodiversity (Sica et al., 2016). The  
61 Ñeembucú Wetlands Complex has a humid subtropical climate, with 1604mm average  
62 total annual precipitation and follows a dry/wet season trend (Beck et al., 2018;  
63 Climate-Data, 2021). Ñeembucú is the 3<sup>rd</sup> least populated department in Paraguay, and  
64 livelihoods within this department predominantly rely on agriculture and local fisheries

65 (UNFPA and DGEEC, 2021). Local populations are dependent on the ecosystem health  
66 of the wetlands as a result. Common agricultural practices in the area include the use of  
67 fire to promote growth of palatable grasses and subsistence deforestation.

68 Utilisation of monitoring to understand wetland dynamics and land use change trends is  
69 crucial for effectively informing decision-making and development planning in the  
70 Ñeembucú Wetlands Complex. Wetland monitoring is important for assessing global  
71 change, identifying areas at high risk of land conversion and degradation, and  
72 examining the effectiveness of policy in preserving wetland habitats (Lang and  
73 McCarty, 2008; Dewan and Yamaguchi, 2009). Knowledge of the pace and extent of  
74 wetland change can be gained using remote sensing techniques and this understanding  
75 is required to effectively manage wetland resources and development. Remote sensing  
76 enables studies on greater spatial and temporal scales and is less expensive than field  
77 studies (Kandus et al., 2018). However, wetland monitoring using remote sensing has  
78 faced challenges as wetland habitats are highly variable and lack unifying features  
79 which enable identification (Gallant, 2015). Recent developments in remote sensing  
80 technology have allowed advancements in wetland delineation, mapping and  
81 monitoring with high-quality, high-resolution satellite imagery (Junk, 2013). In  
82 particular, optical data is limited in its ability to detect hydrology and a shift in data  
83 sources for wetland mapping to synthetic aperture radar data has been seen with the  
84 availability of the Sentinel-1 collection (Guo et al., 2017). Recent developments can be  
85 utilised to gain knowledge about wetland dynamics in the Ñeembucú Wetlands  
86 Complex.

87 The objectives of this study are to use remotely sensed data to map land cover between  
88 2006 and 2021, use these maps to quantify wetland change over the 15-year study  
89 period and thus identify land cover types vulnerable to change in the Ñeembucú  
90 Wetlands Complex.

91

## 92 **2. Materials and Methods**

93 Land cover was identified and quantified for a series of years within a 15-year period  
94 from 2006 to 2021. A two-step classification process was followed; step 1 identified  
95 forest, non-forest vegetation, and open water cover, and step 2 identified dryland

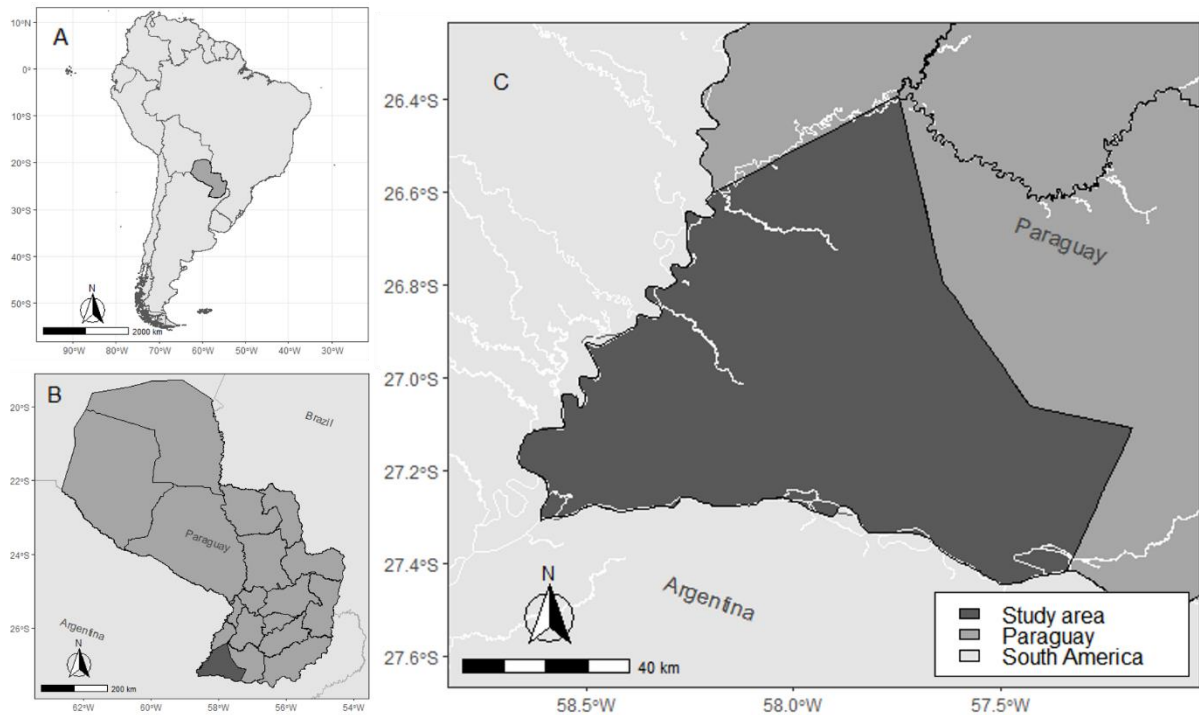
96 vegetation and wetland vegetation, differentiated within the vegetation class from step  
97 1.

98 Forest was defined using the national forest definition, characterised by the presence of  
99 trees and at least 10% canopy cover (FAO, 2020). Vegetated wetland included all  
100 seasonal and permanent wetland types except open water, and this primarily consisted  
101 of freshwater marshes, peatland, seasonally-inundated grassland and shrub-dominated  
102 wetland in the study area (Ramsar, 1990). Dryland was dry vegetation with less than  
103 10% canopy cover from trees, and open water was areas of water not covered by  
104 vegetation.

105 Supervised classifications were carried out for four ‘supervision years’; 2006, 2011,  
106 2016 and 2021. Three further ‘intermediate years’ (2009, 2014 and 2019) were  
107 classified using the classifier trained on the nearest ‘supervision year’. The area covered  
108 by each land cover class was quantified for each year and change over the study period  
109 was measured.

## 110 **2.1 Study Area**

111 The study area is an 8,361km<sup>2</sup> region within the Department of Ñeembucú, Paraguay  
112 (see Figure 1). The study area is bordered by the River Tebicuary in the north, River  
113 Paraguay in the west, River Parana in the south and the department’s administrative  
114 boundary in the east. The Ñeembucú Wetlands Complex is located at the confluence of  
115 two of South America’s most important rivers, the Paraguay and the Paraná, and is part  
116 of the Rio de la Plato Basin System (ymin: -27.44417, ymax: -26.39394, xmin: -  
117 58.66491, xmax: -57.18209). Ñeembucú has the 3<sup>rd</sup> lowest population size of  
118 Paraguay’s departments (UNFPA and DGEEC, 2021).



119

120 *Figure 1. A study area map showing; A the location of Paraguay within South America,*  
121 *B the location of the study area within Paraguay, and C the study area locally. Maps*  
122 *were created using RStudio, and the Paraguay administrative boundaries were sourced*  
123 *from UNFPA and DGEEC (2021) (R Core Team, 2021).*

## 124 **2.2 Datasets**

### 125 **2.2.1 Validation Data**

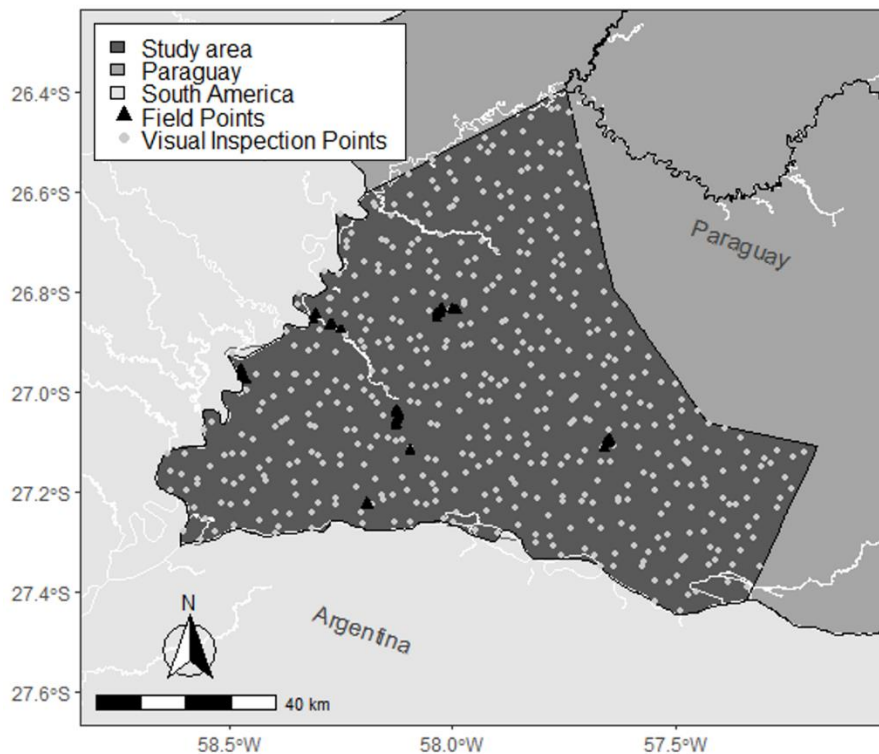
#### 126 **Field Data**

127 Field data was collected in October 2021 from 129 plots within 11 localities across the  
128 study area (See Figure 2). The localities were selected due to being either being public  
129 access land, properties for sale with surveying permissions from the owner, or  
130 properties that we had previously established relationships and permission to survey the  
131 property. Random allocation of plots for field data collection was not feasible for the  
132 study area due to the high proportion of privately owned land (Fian International, 2021).  
133 Between 5 and 21 plots were visited at each locality, depending on locality size. Each  
134 plot is 10m<sup>2</sup> and the plots were distributed evenly across habitat types in each locality  
135 and at least 100m apart. Each plot was recorded as dryland, vegetated wetland or forest.  
136 The forest plots were excluded from the dataset and 97 sample plots remained as field  
137 data to be used in producing a non-forest vegetation classification. The dataset was

138 randomly split into a training partition (75% of observations) and a testing partition  
139 (25% of observations).

#### 140 **Visual Inspection Data**

141 Image interpretation data was collected using Sentinel and Landsat images from  
142 October in supervision years: 2006, 2011, 2016 and 2021 (Copernicus, 2021; USGS,  
143 2021). This was done by visually inspecting 504, randomly allocated, 30m<sup>2</sup> plots on  
144 true colour image composites from the available satellite imagery for October of that  
145 year. Resolutions ranged between 10m<sup>2</sup> and 30m<sup>2</sup> (See Figure 2). The visual inspection  
146 plots were allocated across the study area using random stratified sampling using the  
147 ‘sp’ package v.1.4 in RStudio version 3.7.2 (Pebesma and Bivand, 2005; R Core Team,  
148 2021). For 2006 and 2011, Landsat 7 Surface Reflectance and Landsat 5 Surface  
149 Reflectance were used to create composite images for inspection. For 2016 and 2021,  
150 Sentinel-2 Surface Reflectance and Landsat 8 Surface Reflectance were used to create  
151 composite images for inspection. One composite image from each dataset was produced  
152 for each year, and every sample point was inspected and identified as forest, non-forest  
153 vegetation or open water based on the plot’s appearance. Forest appeared dark green,  
154 open water appeared black or blue, and non-forest vegetation belonged to neither of the  
155 aforementioned classes. Vegetated wetland and dryland could not be differentiated  
156 through a visual inspection because of the high variability and inconsistency in  
157 appearance (Kandus et al., 2018). The visual inspection dataset was randomly split into  
158 a training partition (75% of observations) and a testing partition (25% of observations).



159

160 *Figure 2. A map showing the distribution of ground-truth data used to supervise the*  
161 *land cover classifications. Both groups of points were split randomly into a 75%*  
162 *training partition and 25% testing partition. The visual inspection points ( $n = 504$ )*  
163 *supervised the Level 1 classification and the field points ( $n = 129$ ) supervised the Level*  
164 *2 classification.*

### 165 **2.2.2 Classification Data**

166 Images from the USGS Landsat Collections (Landsat 5, 7 and 8, Level 2 [Collection 2])  
167 and Sentinel Collections (Sentinel-1 SAR GRD and Sentinel-2 MSI) were sourced using  
168 Google Earth Engine for the study period between 2006 and 2021 (Gorelick et al., 2017;  
169 Copernicus, 2021; USGS, 2021).

### 170 **2.3 Identification of land cover**

171 Imagery from the LANDSAT and Sentinel missions were utilised to develop supervised  
172 classifications of land cover over the study period (Copernicus, 2021; USGS, 2021). A  
173 two-step methodology was employed to firstly identify open water, vegetation, and  
174 forest (Level 1 classification), and secondly to identify dryland and vegetated wetland  
175 within the vegetation class (Level 2 classification).

#### 176 **2.3.1 Data processing**



177 Imagery from the Landsat and Sentinel missions over a 12-week period (23<sup>rd</sup> August –  
178 14<sup>th</sup> November) were used to calculate Enhanced Vegetation Index (EVI), Normalized  
179 Difference Vegetation Index (NDVI), Normalized Difference Water Index (NDWI)  
180 from Landsat data and the 10<sup>th</sup> percentile, 90<sup>th</sup> percentile and difference between the 10<sup>th</sup>  
181 and 90<sup>th</sup> percentile for Sentinel-1 bands. The annual seasonality of NDVI, NDWI and  
182 Bare Soil Index (BSI) were calculated over the year leading up to the end date of the 12-  
183 week imagery period. The mean value of bands in each pixel were used to produce a  
184 composite image of the study area. SRTM Digital Elevation Data was also collated at  
185 90m<sup>2</sup> and a mean taken for each 30m<sup>2</sup> pixel of the composite image (Jarvis et al., 2008).  
186 The final composites for each year contained raw bands and processed bands (see Table  
187 1). The equations used in band processing are as follows;

188 For NDVI:

$$189 \quad NDVI = \frac{(NIR-Red)}{(NIR+Red)} \quad (\text{Huete et al., 2002})$$

190

191

192 For NDWI:

$$193 \quad NDWI = \frac{(NIR-SWIR)}{(NIR+SWIR)} \quad (\text{Gao, 1996})$$

194

195 For BSI:

$$196 \quad BSI = \frac{((Red+SWIR)-(NIR+Blue))}{((Red+SWIR)+(NIR+Blue))} \quad (\text{Chen et al., 2004})$$

197

198 For EVI:

$$199 \quad EVI = 2.5 \times \frac{(NIR-Red)}{(NIR+6 \times Red - 7.5 \times Blue + 1)} \quad (\text{Huete et al., 2002})$$

200 **Table 1. Datasets and image bands used in the classification of land cover**

Year	Dataset	Raw Bands	Bands	Dates
------	---------	-----------	-------	-------



2021	Sentinel-1	VV, VH	VV p10, VV p90, VV p10-p90 difference, VH p10, VH p90, VH p10-p90 difference	23/08/21-14/11/21
	Sentinel-2 SR	B1, B2, B3, B4, B5, B6, B7, B8, B8A, B9, B10, B11, B12, BQA	EVI, NDVI, NDWI  Seasonality: NDVI magnitude, phase and mean, NDWI magnitude, phase and mean	23/08/21-14/11/21  Seasonality bands: 14/11/20-14/11/21
	Landsat 7 SR	RGB	Entropy	23/08/21-14/11/21
	SRTM Digital Elevation Data Version 4	Elevation		23/08/21-14/11/21
2016	Landsat 7 SR	B1, B2, B3, B4, B5, B7	EVI, NDVI, NDWI, Entropy	23/08/16-14/11/16
	Landsat 7 TOA	B1, B2, B3, B4, B5, B6 VCID 1, B6 VCID 2, B7, B8, BQA	Seasonality: NDVI magnitude, phase and mean, NDWI magnitude, phase and mean, BSI magnitude, phase and mean	23/08/16-14/11/16  Seasonality bands: 14/11/15-14/11/16
	Landsat 8 SR	B1, B2, B3, B4, B5, B6, B7	EVI, NDVI, NDWI	23/08/16-14/11/16
	Landsat 8 TOA	B1, B2, B3, B4, B5, B6, B7, B8, B9, B10, B11, BQA		23/08/16-14/11/16

	SRTM Digital Elevation Data Version 4	Elevation		23/08/16- 14/11/16
2011	Landsat 7 SR	B1, B2, B3, B4, B5, B7	EVI, NDVI, NDWI, Entropy	23/08/11- 14/11/11
			Seasonality: NDVI magnitude, phase and mean, NDWI magnitude, phase and mean, BSI magnitude, phase and mean	Seasonality bands: 14/11/10- 14/11/11
	Landsat 7 TOA	B1, B2, B3, B4, B5, B6 VCID 1, B6 VCID 2, B7, B8, BQA		23/08/11- 14/11/11
	SRTM Digital Elevation Data Version 4	Elevation		23/08/11- 14/11/11
2006	Landsat 7 SR	B1, B2, B3, B4, B5, B7	EVI, NDVI, NDWI, Entropy	23/08/06- 14/11/06
			Seasonality: NDVI magnitude, phase and mean, NDWI magnitude, phase and mean, BSI magnitude, phase and mean	Seasonality bands: 14/11/05- 14/11/06
	Landsat 7 TOA	B1, B2, B3, B4, B5, B6 VCID 1, B6 VCID 2, B7, B8, BQA		23/08/06- 14/11/06
	Landsat 5 SR	B1, B2, B3, B4, B5, B6, B7, sr_atmos_opacity	EVI, NDVI, NDWI	23/08/06- 14/11/06
	Landsat 5 TOA	B1, B2, B3, B4, B5, B6, B7, BQA		23/08/06- 14/11/06

---

SRTM Digital	Elevation	23/08/06-
Elevation Data		14/11/06
Version 4		

---

201

### 202 **2.3.2 Classification**

203 For the Level 1 classification, which identified open water, vegetation, and forest, a  
204 random forest classifier, with 800 trees, a minimum leaf population of 1 and a bag  
205 fraction of 0.5, was trained using the training partition of visual inspection data. A  
206 supervised classification was performed for each study year (2006, 2011, 2016, 2021),  
207 creating a classification of forest, vegetation and open water for each year. In order to  
208 produce a Level 1 classification for three intermediate years (2009, 2014, 2019), the  
209 trained classifier of the closest year was used to classify the composite image of the  
210 intermediate year. For example, a classification for 2009 was produced using the  
211 classifier trained on 2011 data. A classification for 2014 used the 2016-trained classifier  
212 and a classification for 2019 used the 2021-trained classifier. This produced a  
213 classification of forest, vegetation, and open water for 7 study years between 2006 and  
214 2021. There was no satellite imagery available for 35.8km<sup>2</sup>, 0.4% of the study area, in  
215 the 2021 study period. These pixels were assumed not to have changed since 2020 and  
216 were assigned values from the 2020 classification.

217 For the Level 2 classification, identifying dryland and vegetated wetland, a random  
218 forest classification, with 400 trees, a minimum leaf population of 1 and a bag fraction  
219 of 0.75, was trained using the training partition of the field data. A supervised  
220 classification was performed on the area classified as vegetation in the Level 1  
221 classification for each study year (2006, 2011, 2016, 2021), creating a vegetation type  
222 classification. The same three intermediate years classified in the Level 1 classification  
223 underwent vegetation type classification.

224 The Level 2 classification was combined with the Level 1 classification image for each  
225 study year, producing classified land cover images showing forest, non-forest dryland,  
226 vegetated wetland and open water. Land cover classifications are in 30m<sup>2</sup> resolution and  
227 use a WGS84 coordinate reference system.

### 228 **2.3.3 Accuracy assessment**

229 To assess the accuracy of each classification, a confusion matrix carried out on Google  
230 Earth Engine (Stehman, 1997; Gorelick et al., 2017). A further accuracy assessment was  
231 carried out in RStudio, which quantified the total accuracy of each classification and the  
232 number of false positives and number of false negatives for each class (R Core Team,  
233 2021).

234 Accuracy assessments were carried out for the land cover maps in supervision years,  
235 which were 2006, 2011, 2016, and 2021. These were carried out on the Level 1  
236 classification outputs and Level 2 classification outputs separately.

#### 237 **2.4 Change Detection**

238 The area covered by each land cover class was measured from the land cover  
239 classification for each study year and the mean annual change between each of the  
240 images was calculated. The mean annual change for the whole study period was  
241 calculated by taking the mean of annual change estimates between study years.

#### 242 **2.5 Precipitation Trend**

243 Precipitation data was sourced from the CHIRPS daily (version 2.0) climate dataset at  
244 5566m resolution (Funk et al., 2015). The total annual precipitation was quantified by  
245 taking the sum of total annual precipitation of all pixels across the study area for every  
246 year between 2006 and 2021 on Google Earth Engine (Gorelick et al., 2017). The total  
247 annual precipitation was then plotted using RStudio (R Core Team, 2021).

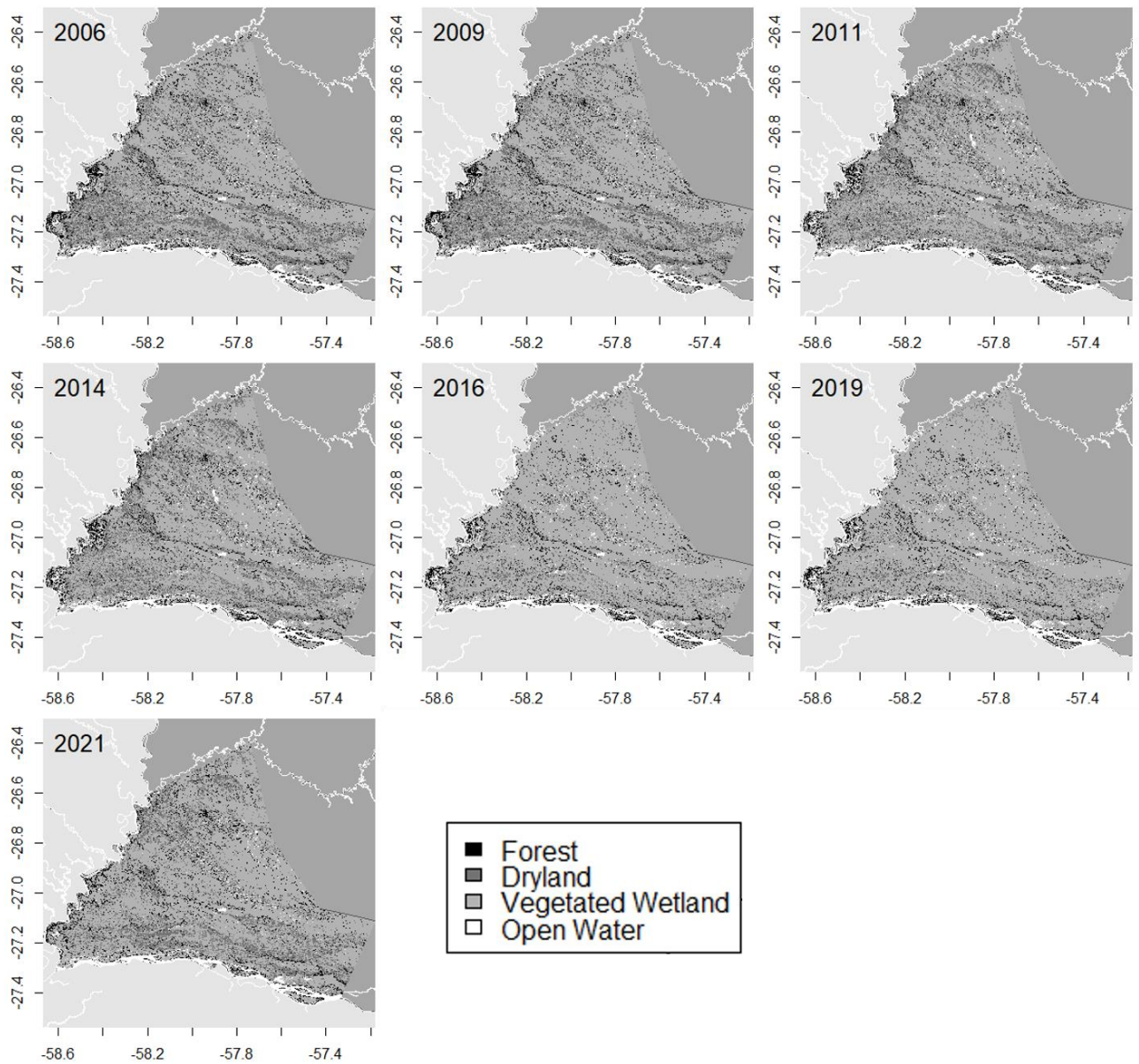
248

### 249 **3. Results**

#### 250 **3.1 Land Cover Classification**

251 Classified land cover maps of the study area, produced in the two-step classification  
252 methodology, are presented in Figure 3. The Ñeembucú Wetlands Complex is  
253 dominated by vegetated wetland, covering 65-79% of the study area between 2006 and  
254 2021. Second to vegetated wetland was dryland, covering 8-23% of the study area over  
255 the study period. In 2016, vegetated wetland covered 11% more of the study area than  
256 for the same class in 2014. Inversely, dryland covered 11% less of the study area than  
257 for the same class in 2016. This is explained by severe flooding due to repeated heavy  
258 rainfall in 2015-2016, which was reported in the Paraguay River basin (Dos-Gollin et  
259 al., 2018). After excluding 2016 observations due to extreme weather, vegetated  
260 wetland and dryland covered 65-70% and 19-23% of the study area, respectively,

261 between 2006 and 2021. Forest and open water covered 6-8% and 5-7% of the study  
262 area, respectively, over the study period.



263

264 *Figure 3. Classified land cover maps of the study area for study years between 2006*  
265 *and 2021. The supervised classification years were 2006, 2011, 2016 and 2021. 2009,*  
266 *2014 and 2019 were intermediate years, classified by the closest years classifier.*  
267 *Classifications created on Google Earth Engine and plotted in RStudio (Gorelick et al.,*  
268 *2017; R Core Team, 2021).*

### 269 **3.2 Classification Accuracy Assessment**

270 The random forest classification produced Level 1 land cover classification maps with  
271 91-96% overall accuracies and Level 2 land cover classification maps with an 82%

272 overall accuracy. Table 2 presents the overall accuracy, and percentage of false  
 273 negatives (Type I errors) and false positives (Type II errors) in each land cover class in  
 274 supervision years (the years in which training and testing data were available to  
 275 supervise classifications).

276 Within the Level 1 Classification, vegetation was overrepresented for all years. Forest  
 277 was the most underrepresented class in all years, with false negatives ranging between  
 278 2.9% of test observations in 2021 and 4.7% in 2011. In 2006, 0.8% and 3.1% of open  
 279 water and forest observations, respectively, were falsely identified as vegetation. In  
 280 2011, over two thirds of the vegetation false positives were classified as forest in the  
 281 testing data, and the remaining were open water. The proportion of vegetation false  
 282 positive belonging to forest and open water was similar to in 2011, with over two thirds  
 283 of the vegetation false positives classified as forest in the testing data. In 2021, no errors  
 284 were identified in the open water class, and there was a 0.7% greater false positive  
 285 identification of vegetation than of forest.

286 The Level 2 classification had a lower accuracy than the Level 1 classification, due to  
 287 the heterogeneity in habitat types within non-forest vegetation leading to a lack of  
 288 unifying features within classes (Gallant, 2015). Within both dry and wetland  
 289 vegetation, dominance of grasses, herbaceous plants and shrubs vary, and the  
 290 seasonality of water presence varies within the vegetated wetland class too. Within the  
 291 Level 2 classification, dryland was overrepresented, with a greater number of false  
 292 positives than the vegetated wetland class.

293 **Table 2. The accuracy of each classification in identifying each land cover**

Level 1 Land Cover Classification							
Year	Overall Classifier Accuracy (%)	Forest		Vegetation		Open Water	
		False Positive (%)	False Negative (%)	False Positive (%)	False Negative (%)	False Positive (%)	False Negative (%)
2006	96	0	3.1	3.9	0	0	0.8
2011	91	1.6	4.7	6.3	2.3	1.6	2.3
2016	94	0.8	3.1	3.8	2.3	1.5	0.8
2021	95	2.2	2.9	2.9	2.2	0	0



Level 2 Land Cover					
Classification					
Year	Overall Classifier Accuracy (%)	Dryland		Vegetated Wetland	
		False Positive (%)	False Negative (%)	False Positive (%)	False Negative (%)
2021	82	10.7	7.1	7.1	10.7

294

### 295 3.3 Land Cover Change Detection

296 The greatest annual change throughout the study period was observed in the dryland  
 297 vegetation and vegetated wetland land cover classes (see Table 3). Extreme change in  
 298 dryland and vegetated wetland was seen between 2014 and 2016, with changes of -  
 299 65.76% and 7.72% observed in each class, respectively. The extreme figures observed  
 300 in 2016 are the results of extreme weather, and this year's classification was removed  
 301 from the change detection as a result (Dos-Gollin et al., 2018; Figure 4). The change  
 302 detection showed vegetated wetlands decreasing at a mean annual rate of 1.65%, and a  
 303 mean annual increase in dryland of 4.94% (Table 3). Further to this, forest is lost at a  
 304 rate of 0.34% annually, while open water is gained at a mean rate of 0.40% annually.

305 **Table 3. Mean annual change (%) in area in each land cover between study years**

Time Period	Forest	Dryland	Vegetated Wetland	Open Water
2006-2009	-9.12	3.89	-0.92	3.37
2009-2011	9.00	-9.69	1.80	1.34
2011-2014	3.54	-1.13	-0.52	4.42
2014-2019	-3.70	1.54	0.13	-3.07
2019-2021	-1.43	30.07	-8.74	-4.07
Overall Study Period	-0.34	4.94	-1.65	0.40

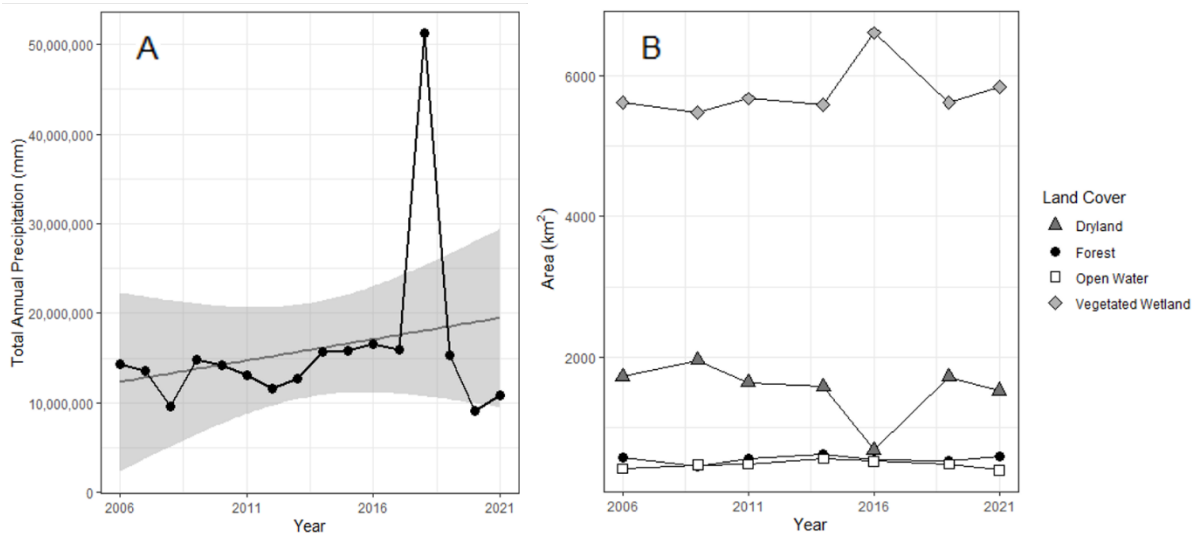
306

### 307 3.4 Precipitation Trend

308 Total annual precipitation ranged between 9,036,984mm and 16,546,476mm and  
 309 displayed an increasing trend over the study period (see Figure 4). However, greater  
 310 variability in annual precipitation is seen in the latter years within the study period, with



311 total annual precipitation more than three times greater than the previous year observed  
312 in 2016, and some of the lowest rainfall years observed in 2020 and 2021 (Figure 4a).  
313 The impact of extreme precipitation in 2016 is observed in the inundation of a greater  
314 area of non-forested land in that year (Figure 4b).



315

316 *Figure 4. Temporal pattern of A total annual precipitation (mm) and B area (km<sup>2</sup>)*  
317 *under each land cover class in the study area between 2006 and 2021. In A, the*  
318 *observed annual precipitation is plotted in black and the fitted precipitation trend in*  
319 *grey. Sources: The CHIRPS daily (version 2.0) climate dataset (Funk et al., 2015).*  
320 *Processed in Google Earth Engine and plotted in RStudio (Gorelick et al., 2017; R*  
321 *Core Team, 2021).*

322

#### 323 **4. Discussion**

324 The wetland change identified in the Ñeembucú Wetlands Complex is comparable to  
325 wetland change reported in regions of the Paraguay-Paraná-La Plata River system,  
326 where pressure from human activities events is driving wetland conversion and  
327 degradation trends (Collischonn et al., 2001; Junk, 2013). In the Lower Paraná River  
328 Delta, one third of freshwater marshes were converted to pasture and forestry between  
329 1999 and 2013 (Sica et al., 2016). Similarly, Guerra et al. (2020) projected a 3% loss in  
330 native vegetation by 2050 in the Pantanal, the lowland region of the Upper Paraguay  
331 River Basin. Brandolin et al. (2013) found a 15% loss in flooded area in Córdoba,  
332 Argentina, and area in which agricultural expansion has driven high channelisation of  
333 the wetlands between 1987 and 2007. Conversely, a 66% increase in flooded area was

334 seen in Santa Fe, a region experiencing lower agricultural pressure, within the same  
335 study in Argentina. The increase in flooded area observed in Santa Fe was attributed to  
336 increased flooding driving expansion of wetlands in a region with low agricultural  
337 pressure (Brandolin et al., 2013). The findings of this study suggest that wetland areas  
338 within the Ñeembucú Wetlands Complex are being converted to dryland, a similar trend  
339 observed in other regions within the Paraguay-Paraná-La Plata River system, and  
340 globally (Kashaigili et al., 2006; Junk, 2013; Gardner et al., 2015).

341 Land use in the Ñeembucú Wetlands Complex is predominantly agricultural and it is  
342 likely that agricultural and urban expansion is driving the drainage and conversion of  
343 wetlands to dryer, productive lands (Bucher & Huszar, 1995; JICA-CEPAL, 2013). This  
344 trend is seen in wetlands both globally and within the Paraguay-Paraná-La Plata River  
345 system. Wetland loss in the Ñeembucú Wetlands Complex is comparable to that seen in  
346 Argentina, where the use of water management infrastructure, such as channels and  
347 levees, has been held responsible for driving wetland conversion (Bucher and Huszar,  
348 1995; Brandolin et al., 2013; Sica et al., 2016). In wetlands with high agricultural  
349 production in the Paraná River Delta in Argentina, artificial drainage channels were  
350 constructed to mitigate the impacts of frequent flooding caused by an increasing rainfall  
351 trend in the latter half of the 20<sup>th</sup> century, and illegal construction of channels by  
352 landowners followed (Brandolin et al., 2013). Within the Lower Paraná River Delta,  
353 water management practices, cattle density, and accessibility were the primary drivers  
354 of wetland conversion (Brandolin et al., 2013; Sica et al., 2016). In the Upper Paraguay  
355 River Basin, native vegetation loss was driven by commodity agriculture, protection  
356 status, and accessibility (Guerra et al., 2020). The relative influences of these variables  
357 differed spatially, with agriculture having a lesser effect and distance to roads having a  
358 greater effect in the Pantanal wetlands compared to the dryer surrounding Cerrado and  
359 Amazon biomes.

360 Wetland conversion observed in the Ñeembucú Wetlands Complex is likely not  
361 attributed to precipitation, as total annual precipitation and extreme precipitation trends  
362 are increasing in the region. Doyle and Barros (2011) found increasing precipitation  
363 localised to both the Middle Paraná and Middle Paraguay Basins, in which the  
364 Ñeembucú Wetlands Complex lies, and Haylock et al. (2006) reported increased annual  
365 precipitation and extreme precipitation days, with a shortened wet season, for Paraguay  
366 and the surrounding region. Further to this, an increasing trend was seen for total annual

367 precipitation in the Ñeembucú Wetlands Complex, within this study. Wetland dynamics  
368 are largely driven by precipitation, and without simultaneous urban and agricultural  
369 development, increasing precipitation is expected to drive greater inundation and  
370 flooding (Collischonn et al., 2001; Prieto, 2007; Pereira et al., 2021). The  
371 aforementioned increasing inundation observed in Santa Fe, Argentina, is an example of  
372 wetland expansion driven by increasing precipitation (Brandolin et al., 2013). The  
373 precipitation trends observed in the study area and the surrounding region suggest  
374 climate change is not driving conversion of wetlands observed in this study.

375 Continued loss of vegetated wetlands and forest in the Ñeembucú Wetlands Complex  
376 will reduce the capacity of the ecosystem to provide valuable goods and services,  
377 including water storage, provisioning of fish and fuel, and supporting wetland  
378 biodiversity. Recent developments in the region including the Coastal Defences of Pilar  
379 and Alberdi-Pilar Ruta constructions pose a further threat this vulnerable habitat  
380 (Gardner et al., 2015; MOPC, 2021a; MOPC, 2021b). The primary goals of these  
381 developments are to alleviate flood risk and increasing accessibility to Ñeembucú's  
382 main city, Pilar, which are frequently acknowledged as drivers of wetland conversion.  
383 Further to this, development of the floodplain in Ñeembucú may reduce water storage  
384 and drive flooding in the rest of the region (Gottgens et al., 2001). It may also be the  
385 case that land use change and river modifications upstream of the Ñeembucú Wetlands  
386 Complex are influencing wetland change by moderating river discharges (da Silva and  
387 Girard, 2004). Given the clear impact global change has already had on these wetlands,  
388 wetland monitoring is an essential tool for preserving the economic, ecological and  
389 cultural value of the Ñeembucú Wetlands Complex (Sica et al., 2016; Kandus et al.,  
390 2018; Guerra et al., 2020).

391 Continued monitoring of the Ñeembucú Wetlands Complex and further analysis of the  
392 drivers of land use change in the region are essential for well-informed decision-making  
393 in the region (Junk, 2013; Guo et al., 2017; Kaplan and Avdan, 2018). Globally, the  
394 value of wetlands has rarely been seriously considered within decision-making  
395 (Woodward and Wui, 2001). However, integration of the value of wetlands into  
396 decision-making and development-planning will promote conservation of economically,  
397 ecologically, and culturally valuable wetland habitats. Further analysis of change within  
398 wetland types, and the drivers of this change, will be essential for identifying vulnerable  
399 habitats, monitoring wetland health and understanding the role of policy and

400 development in driving wetland dynamics in Ñeembucú (Gumbricht et al., 2017;  
401 Davidson & Finlayson, 2018).

402

## 403 **5. Conclusion**

404 With around 6000km<sup>2</sup> of wetland area within an 8000km<sup>2</sup> complex of forest, grassland  
405 and wetland, the Ñeembucú Wetlands Complex is a valuable region within the  
406 Paraguay-Paraná-La Plata River system within which preservation of biodiversity,  
407 provisioning of natural resources, and water storage must be considered within  
408 development process. Within the Ñeembucú Wetlands Complex, vegetated wetlands  
409 and forest have been lost over the last 15 year, predominantly being converted into more  
410 productive, dryland areas. Given the increasing precipitation trends identified in the  
411 region, it's likely that agricultural and urban development is driving land use change in  
412 the region. With large, ongoing, developments in the region, continued monitoring will  
413 be essential for understand the impact on the Ñeembucú Wetlands Complex, a region in  
414 which much of the population's livelihoods depend on ecosystem health. With current  
415 ongoing developments in the area and projected continued climatic and anthropogenic  
416 pressures, monitoring will be essential for understanding the impact of climate change  
417 and development on wetland health. Wetland monitoring is a key tool for addressing  
418 wetland change and gaining the knowledge required for well-informed decision making  
419 around future development and conservation of valuable ecosystem goods and services.

420

## 421 **Acknowledgements**

422 I would like to thank Fundación Para La Tierra for their support throughout this study  
423 and, in particular, to Jorge Ayala, Jack Haines, Sol Gomez, Cristian Torres and Ellen  
424 Brogan for logistical and fieldwork assistance. I am grateful to the landowners that gave  
425 us permission to survey properties across Ñeembucú.

426

## 427 **Conflict of Interest Statement**

428 The authors declare no conflicts of interest

429

430 **Declaration of Funding**

431 This research did not receive any specific funding

432

433 **Data Availability Statement**

434 The data that support this study will be shared upon reasonable request to the  
435 corresponding author.

436

437 **References**

438 Baker, C., Lawrence, R., Montagne, C., Patten, D. (2007). Change Detection of  
439 Wetland Ecosystems Using Landsat Imagery and Change Vector Analysis. *Wetlands*  
440 **27(3)**, 610-619.

441 Beck, H., Zimmermann, N., McVicar, T., Vergopolan, N., Berg, A., Wood, E. F.  
442 (2018). Present and future Köppen-Geiger climate classification maps at 1-km  
443 resolution. *Scientific Data* **5**, 180214.

444 Brandolin, P. G., Ávalos, M. A., De Angelo, C. (2013). The impact of flood control on  
445 the loss of wetlands in Argentina. *Marine and Freshwater Research* **23**, 291-300.

446 Bucher, E. Huszar, P. (1995). Critical environmental costs of the Paraguay-Paraná  
447 waterway project in South America. *Ecological Economics* **15**, 3-9.

448 Chen, W., Liu, L., Zhang, C., Wang, J., Wang, J., Pan, Y. (2004). Monitoring the  
449 seasonal bare soil areas in Beijing using multi-temporal TM images. *International*  
450 *Geoscience and Remote Sensing Symposium* **5**, 3379–3382.

451 Collischonn, W., Tucci, C., Clarke, R. (2001). Further evidence of changes in the  
452 hydrological regime of the River Paraguay: part of a wider phenomenon of climate  
453 change? *Journal of Hydrology* **245**, 218-238.

454 Copernicus Sentinel data. (2021). Available online:  
455 <https://developers.google.com/earth-engine/datasets/catalog/sentinel>

456 Climate-Data. (2021). ‘Climate Pilar (Paraguay)’. Available at: [https://en.climate-](https://en.climate-data.org/south-america/paraguay/neembucu/pilar-3863/)  
457 [data.org/south-america/paraguay/neembucu/pilar-3863/](https://en.climate-data.org/south-america/paraguay/neembucu/pilar-3863/) [accessed 29 December 2021].

- 458 Davidson, N., Finlayson, C. (2018). Extent, regional distribution and changes in area of  
459 different classes of wetland. *Marine and Freshwater Research* **69(10)**, 1525-1533.
- 460 Dewan, A., Yamaguchi, Y. (2009). Using remote sensing and GIS to detect and monitor  
461 land use and land cover change in Dhaka Metropolitan of Bangladesh during 1960–  
462 2005. *Environmental Monitoring and Assessment* **150**, 237–249.
- 463 Dos-Gollin, J., Muñoz, Á. G., Mason, S. J., Pastén, M. (2018). Heavy Rainfall in  
464 Paraguay during the 2015/16 Austral Summer: Causes and Subseasonal-to-Seasonal  
465 Predictive Skill. *Journal of Climate* **31(17)**, 6669–6685.
- 466 Doyle, M. E., Barros, V. R. (2011). Attribution of the river flow growth in the Plata  
467 Basin. *International Journal of Climatology* **31**, 2234-2248.
- 468 FAO. (2020). Global Forest Resource Assessment – Paraguay. Available at:  
469 <https://www.fao.org/forest-resources-assessment/fra-2020/country-reports/en/> [accessed  
470 28 December 2021].
- 471 Fian International. (2021). ‘Paraguay: Stop the wave of forced evictions and  
472 criminalisation of peasant and indigenous communities’. Available at:  
473 [https://www.fian.org/en/press-release/article/paraguay-stop-the-wave-of-forced-](https://www.fian.org/en/press-release/article/paraguay-stop-the-wave-of-forced-evictions-and-criminalization-of-peasant-and-indigenous-communities-2894)  
474 [evictions-and-criminalization-of-peasant-and-indigenous-communities-2894](https://www.fian.org/en/press-release/article/paraguay-stop-the-wave-of-forced-evictions-and-criminalization-of-peasant-and-indigenous-communities-2894) [accessed  
475 29 December 2021].
- 476 Funk, C., Peterson, P., Landsfeld, M., Pedreros, D., Verdin, J., Shukla, S., Husak, G.,  
477 Rowland, J., Harrison, L., Hoell, A., Michaelsen, J. (2015). The climate hazards  
478 infrared precipitation with stations—a new environmental record for monitoring  
479 extremes. *Scientific Data* **2**, 150066.
- 480 Gallant, A. (2015). The Challenges of Remote Monitoring of Wetlands. *Remote Sensing*  
481 **7**, 10938-10950.
- 482 Gao, B. C. (1996). NDWI—A normalized difference water index for remote sensing of  
483 vegetation liquid water from space. *Remote Sensing of Environment* **58**, 257–266.
- 484 Gardner, R. C., Barchiesi, S., Beltrame, C., Finlayson, C., Galewski, T., Harrison, I.,  
485 Paganini, M., Perennou, C., Pritchard, D., Rosenqvist, A., Walpole, M. (2015). State of  
486 the World's Wetlands and Their Services to People: A Compilation of Recent Analyses  
487 (March 31, 2015). In: ‘Ramsar Briefing Note No. 7.’ (Gland, Switzerland: Ramsar

- 488 Convention Secretariat). Available at SSRN: <https://ssrn.com/abstract=2589447> or  
489 <http://dx.doi.org/10.2139/ssrn.2589447>
- 490 Gorelick, N., Hancher, M., Dixon, M., Ilyushchenko, S., Thau, D., & Moore, R. (2017).  
491 Google Earth Engine: Planetary-scale geospatial analysis for everyone. *Remote Sensing*  
492 *of Environment* **202**, 18-27.
- 493 Gottgens, J. F., Perry, J. E., Fortney, R. H., Meyer, J. E., Benedict, M., Rood, B. E.  
494 (2001). The Paraguay–Paraná Hidrovía: Protecting the Pantanal with Lessons from the  
495 Past. *BioScience* **51(4)**, 301-308.
- 496 Guerra, A., Roque, F. O., Garcia, L. C., Ochoa-Quintero, J. M., Tarso, P., Oliveira, S.,  
497 Guariento, R. D., Rosa, I. M. D. (2020). Drivers and projections of vegetation loss in  
498 the Pantanal and surrounding ecosystems. *Land Use Policy* **91**, 104388.
- 499 Gumbrecht, T., Roman-Cuesta, R., Verchot, L., Herold, M., Wittmann, F., Householder,  
500 E., Herold, N., Murdiyarso, D. (2017). An expert system model for mapping tropical  
501 wetlands and peatlands reveals South America as the largest contributor. *Global*  
502 *Change Biology* **23**, 3581–3599.
- 503 Guo, M., Sheng, C., Xu, J., Wu, L. (2017). A Review of Wetland Remote Sensing.  
504 *Sensors* **17**, 777.
- 505 Haylock, M. R., Peterson, T. C., Alves, L. M., Ambrizzi, T., Anunciação, Y. M. T.,  
506 Baez, J., Barros, V. R., Berlato, M. A., Bidegain, M., Coronel, G., Corradi, V., Garcia,  
507 V. J., Grimm, A. M., Karoly, D., Marengo, J. A., Marino, M. B., Moncunill, D. F.,  
508 Nechet, D., Quintana, J., Rebello, E., Rusticucci, M., Santos, J. L., Trebejo, I., Vincent,  
509 L. A. (2006). Trends in Total and Extreme South American Rainfall in 1960–2000 and  
510 Links with Sea Surface Temperature. *Journal of Climate* **19(8)**, 1490–1512.
- 511 Huete, A., Didan, K., Miura, T., Rodriguez, E., Gao, X., Ferreira, L. (2002). Overview  
512 of the radiometric and biophysical performance of the MODIS vegetation indices.  
513 *Remote Sensing of Environment* **83**, 195-213.
- 514 Jarvis, A., Reuter, H. I., Nelson, A., Guevara, E. (2008). Hole-filled SRTM for the  
515 globe Version 4, available from the CGIAR-CSI SRTM 90m Database. Available at:  
516 <https://srtm.csi.cgiar.org> [accessed 30 October 2021].



- 517 JICA-CEPAL. (2013). Study on inclusive development in Paraguay: International  
518 cooperation experiences. Asunción, October 2013. Available at:  
519 [https://www.jica.go.jp/jica-ri/publication/booksandreports/\\_20143j.html](https://www.jica.go.jp/jica-ri/publication/booksandreports/_20143j.html) [accessed 28  
520 December 2021].
- 521 Junk, W. (2013). Current state of knowledge regarding South America wetlands and  
522 their future under global climate change. *Aquatic Sciences* **75**, 113-131.
- 523 Kandus, P., Minotti, P., Morandier, N., Grimson, R., Trilla, G., González, E., Martín,  
524 L., Gayol, M. (2018). Remote sensing of wetlands in South America: status and  
525 challenges. *International Journal of Remote Sensing* **39(4)**, 993-1016.
- 526 Kaplan, G., Avdan, U. (2018). Monthly analysis of wetlands dynamics using remote  
527 sensing data. *International Journal of Geo-Information* **7**, 411.
- 528 Kashaigili, J., Mbilinyi, B., McCartney, M., Mwanuzi, F. (2006). Dynamics of Usangu  
529 plains wetlands: Use of remote sensing and GIS as management decision tools. *Physics  
530 and Chemistry of the Earth* **31**, 967-975.
- 531 Lang, M.W., McCarty, G.W. (2008). Wetland Mapping: History and Trends. In: Russo,  
532 R.E., editor. Wetlands: Ecology, Conservation and Restoration. (Eds Russo, R.E.) pp.  
533 74-112. (Hauppauge, NY: Nova Science Publishers).
- 534 Millennium Ecosystem Assessment, 2005. Ecosystems and Human Well-Being:  
535 Wetlands and Water. Washington DC.
- 536 Milliman, J. & Meade, R. 1983. World-Wide Delivery of River Sediment to the Oceans.  
537 *The Journal of Geology* **91(1)**, 1-21.
- 538 MOPC. (2021a). ‘Defensa Costera de Pilar’. Available at:  
539 <https://www.mopc.gov.py/index.php/defensa-costera-de-pilar> [accessed 27 December  
540 2021].
- 541 MOPC. (2021b). ‘Noticias’. Available at:  
542 [https://www.mopc.gov.py/index.php/noticias/tag/ruta%20alberdi%20%E2%80%9320  
543 pilar](https://www.mopc.gov.py/index.php/noticias/tag/ruta%20alberdi%20%E2%80%9320pilar) [accessed 27 December 2021].
- 544 Pebesma, E., Bivand R.S. (2005). ‘Classes and methods for spatial data in R.’ *R News*  
545 **5(2)**, 9–13.

- 546 Pereira, G., Ramos, R. C., Rocha, L. C., Nathaniel Alan Brunsell, Merino, E. R.,  
547 Mataveli, A. V., Cardozo, F. S. (2021). Rainfall patterns and geomorphological controls  
548 driving inundation frequency in tropical wetlands: How does the Pantanal flood?  
549 *Progress in Physical Geography: Earth and Environment* **45(5)**.
- 550 Pett, B., Wyer, R. (2020). First confirmed record of the genus *Cybaeodamus* (Araneae:  
551 Zodariidae) in Paraguay, with notes on its distribution. *Revista Ibérica de Aracnología*  
552 **36**, 161-162.
- 553 Prieto, M.d. (2007). ENSO signals in South America: rains and floods in the Paraná  
554 River region during colonial times. *Climatic Change* **83**, 39–54.
- 555 R Core Team (2021). R: A language and environment for statistical computing. R  
556 Foundation for Statistical Computing, Vienna, Austria. URL [https://www.R-](https://www.R-project.org/)  
557 [project.org/](https://www.R-project.org/).
- 558 Ramsar Convention. (1990). Recommendation 4.7: Mechanisms for improved  
559 application of the Ramsar Convention. In: ‘Convention on Wetlands 4th Meeting of the  
560 Conference of the Contracting Parties. Montreux, Switzerland 27 June – 4 July 1990’.  
561 (Ramsar, Iran, 1971).
- 562 Ramsar Convention. (2016). The 4th Strategic Plan 2016 – 2024. (Gland, Switzerland).
- 563 Reis, V., Hermoso, V., Hamilton, S., Ward, D., Fluet-Chouinard, E., Lehner, B., Linke,  
564 S. (2017). A Global Assessment of Inland Wetland Conservation Status. *BioScience*  
565 **67(6)**, 523-533.
- 566 Rosset, V., Bartozek, E., Lambrecht, R., Auricchio, M., Santos, M., Peres, C. (2020).  
567 Gaps and challenges in the knowledge of algal biodiversity in Paraguay. *Phycologia*  
568 **59(6)**.
- 569 da Silva, C. J., Girard, P. (2004). New challenges in the management of the Brazilian  
570 Pantanal and catchment area. *Wetland Ecology and Management* **12**, 553-561.
- 571 Sica, Y., Quintana, R., Radeloff, V., Gavier-Pizarro, G. (2016). Wetland loss due to  
572 land use change in the Lower Paraná River Delta, Argentina. *Science of the Total*  
573 *Environment* **568**, 967-978.
- 574 Slagter, B., Tsendbazar, N., Vollrath, A., Reiche, J. (2020). Mapping wetland  
575 characteristics using temporally dense Sentinel-1 and Sentinel-2 data: A case study in

- 576 the St. Lucia wetlands, South Africa. *International Journal of Applied Earth*  
577 *Observation Geoinformation* **86**, 102009.
- 578 Stehman, S. V. (1997). Selecting and interpreting measures of thematic classification  
579 accuracy. *Remote Sensing of Environment* **62(1)**, 77-89.
- 580 UNFPA and DGEEC (Dirección General de Estadísticas, Encuestas y Censos). (2021).  
581 Paraguay - Subnational Population Statistics – 2021 Projections. Available at:  
582 <https://data.humdata.org/dataset/paraguay-subnational-population-statistics> [accessed:  
583 25 November 2021].
- 584 USGS Landsat data. (2021). Available online: [https://developers.google.com/earth-](https://developers.google.com/earth-engine/datasets/catalog/landsat)  
585 [engine/datasets/catalog/landsat](https://developers.google.com/earth-engine/datasets/catalog/landsat)
- 586 Woodward, R., Wui, Y. (2001). The economic value of wetland services: a meta-  
587 analysis. *Ecological Economics* **37**, 257-270.